Thin Solid Films 676 (2019) 108–112

Contents lists available at ScienceDirect

Thin Solid Films

journal homepage: www.elsevier.com/locate/tsf

Optimizing pyramidal silicon substrates through the electroless deposition of Ag nanoparticles for high-performance surface-enhanced Raman scattering

Tung-Hao Chang[a,b], Yu-Cheng Chang[c,*], Chien-Ming Chen[c], Kai-Wei Chuang[c]

[a] Department of Radiation Oncology, Changhua Christian Hospital, Changhua 50006, Taiwan
[b] Department of Radiological Technology, Yuanpei University, Hsinchu 30015, Taiwan
[c] Department of Materials Science and Engineering, Feng Chia University, Taichung 40724, Taiwan

ARTICLE INFO

Keywords:
Silver
Nanoparticles
Pyramidal silicon
Electroless deposition
Surface-enhanced Raman scattering
5-fluorouracil

ABSTRACT

This work describes the direct fabrication of Ag nanoparticles on pyramidal silicon using a facile, one-step, electroless deposition process at room temperature with short reaction time (3 min). The resulting device could use for rapid drug detection based on surface-enhanced Raman scattering (SERS). The size of the silicon pyramids controlled by altering the texturing time of the silicon substrate. Spin coating was used to enable the rapid deposition of rhodamine 6G molecules (3 min) on the Ag nanoparticles. The resulting pyramidal silicon decorated with Ag nanoparticles provides large specific area as well as hot spots to promote localized surface plasmon resonance, resulting in notable SERS enhancement and a low 5-fluorouracil detection limit (10^{-6} M).

1. Introduction

Texturing the surface of silicon substrates to form pyramidal structures is widely used to increase the light trapping and anti-reflection properties of high-performance solar cells [1–6]. A variety of methods have developed for the fabrication of pyramidal silicon, such as wet chemical etching, dry etching, and electrochemical etching [7–11]. Wet chemical etching generally prefers because it can be achieved at a reasonable cost, at industrial scales, without the need for a template [9,12]. Pyramidal silicon widely uses as an active substrate in surface-enhanced Raman scattering (SERS) due to its unique geometric morphology [13,14]. Pyramidal silicon provides a large surface area, and the structures can be adjusted to increase the number of hot spots, thereby enhancing sensitivity to SERS signals [15,16]. Pyramidal silicon with well-separated arrays easily coat with a uniform layer of Ag or Au nanoparticles via thermal evaporation or ion sputtering; however, those methods are expensive and time-consuming [17–19]. In the present study, we developed an inexpensive, facile electroless deposition method to enable the growth of Ag nanoparticles directly on pyramidal silicon.

The electroless deposition has been studied extensively for the deposition of Ag dendrites on a silicon substrate, due to its simplicity and potential for large-scale manufacturing [20,21]. The electroless deposition could also be used to deposit Ag nanoparticles on silicon nanowires for SERS applications [22,23]. Nonetheless, despite considerable research into the electroless deposition of Ag nanoparticles as a SERS substrate, few researchers have investigated the relationship between the size of the pyramidal structures and the Ag nanoparticles regarding their effects on SERS applications.

2. Experimental

2.1. Synthesis

Pyramidal silicon was fabricated by wet texturing single-crystal silicon wafers in 0.9 M potassium hydroxide (KOH) and 0.64 M aqueous ethanol solution for an appropriate duration. This process facilitated by the anisotropic etching characteristics of single-crystal silicon. Ag nanoparticles were grown on the surface of the pyramidal silicon using electroless plating in 10 mL of aqueous solution containing the concentrations of 8 mM silver nitrate and 90 mM hydrofluoric acid for 3 min. The substrate was then washed using deionized water and ethanol, and dried under air purge.

2.2. Characterization

The morphology of the Ag nanoparticles was examined using a field-emission scanning electron microscope (FESEM, Hitachi S-4800) at a

* Corresponding author.
E-mail address: yuchchang@fcu.edu.tw (Y.-C. Chang).

https://doi.org/10.1016/j.tsf.2019.02.044
Received 30 November 2018; Received in revised form 15 February 2019; Accepted 26 February 2019
Available online 27 February 2019

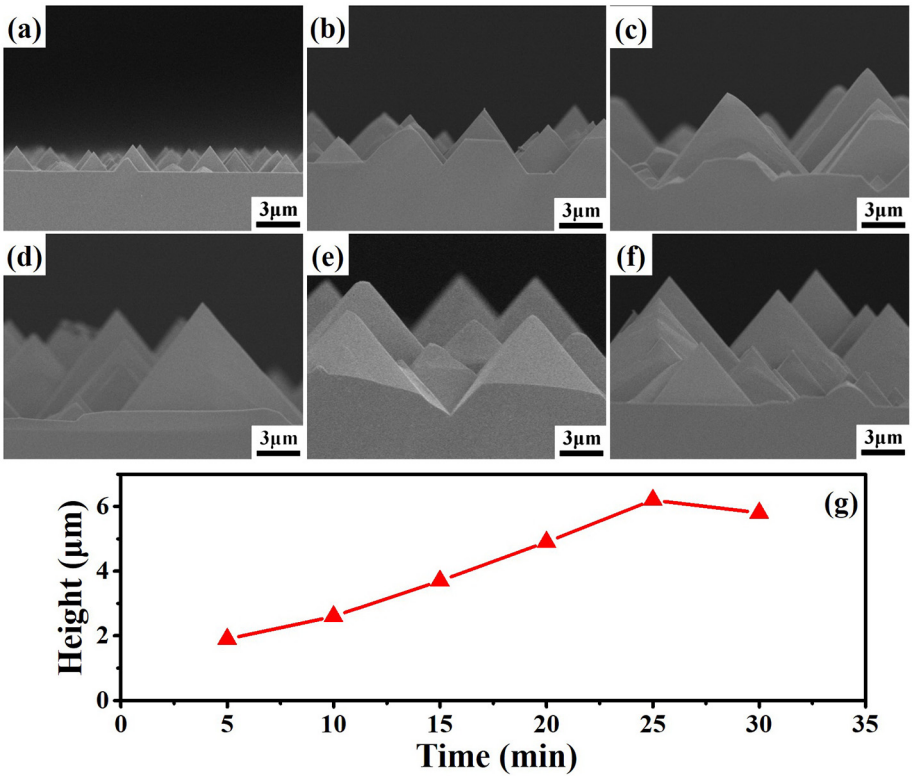

Fig. 1. Cross-sectional SEM images showing pyramidal silicon structures of various size following wet texturing for periods of (a) 5, (b) 10, (c) 15, (d) 20, (e) 25, and (f) 30 min, respectively. (g) The height of pyramidal structures as a function of wet texturing time.

low accelerating voltage (10 kV). The crystalline phase of the Ag nanoparticles was identified using an X-ray diffractometer (XRD, Bruker D2 phaser) with CuKα radiation (λ = 0.154 nm). For prepared TEM sample, Ag nanoparticles were released from the substrate surface by sonicating the as-grown sample in ethanol. A small amount of the suspension of Ag nanoparticles dripped on a carbon-coated copper grid. TEM images were obtained using a field-emission transmission electron microscope (FETEM, JEOL-2100F) at a high accelerating voltage (200 kV). The reflection spectra were obtained using UV–vis spectroscopy (PerkinElmer Lambda 650S). Raman spectra were obtained using a confocal Raman microscope (Protrustech MRI532S, Taiwan) at room temperature in backscattering configuration using a He—Ne laser source with a wavelength of 532 nm.

3. Results and discussion

Figs. 1a–f respectively present cross-sectional SEM images of the pyramid silicon fabricated using 0.9 M of KOH and 0.64 M of ethanol via wet texturing at 80 °C for the different texturing time. The texturing time are (a) 5, (b) 10, (c) 15, (d) 20, (e) 25, and (f) 30 min, respectively. The average heights of the pyramidal structures are 1.9, 2.6, 3.7, 4.9, 6.2, and 5.8 μm, respectively. As shown in Fig. 1g, the height of the pyramidal structures gradually increased with an increase in texturing time, and the highest structures formed after undergoing texturing for 25 min. A further rise in texturing time (30 min) resulted in the destruction of the pyramid structures with a corresponding reduction in height. Ag nanoparticles were then grown on the pyramid silicon by using the electroless deposition in 10 mL of aqueous solution containing an appropriate concentration of silver nitrate (8 mM) and hydrofluoric acid (90 mM) for 3 min. Figs. 2a–f present cross-sectional SEM images showing Ag nanoparticles deposited pyramidal structures of various size (texturing time of (a) 5, (b) 10, (c) 15, (d) 20, (e) 25, and (f) 30 min, respectively). The Ag nanoparticles completely covered the pyramidal silicon, stacking in top area to form Ag dendrites.

Fig. 3a presents a TEM image of an Ag nanoparticle with an oval structure. Fig. 3b displays a high-resolution (HR) TEM image of an Ag nanoparticle with lattice fringe measured at 0.238 nm, which corresponds to the *d*-spacing of the (111) crystal plane of cubic Ag (JCPDS Card No. 04-0783). As shown in Fig. 3c, XRD diffraction was used to characterize the crystal structure, and orientation of the Ag nanoparticles is decorating the pyramid silicon. The crystalline peaks of the Ag nanoparticles observed at the 2θ positions of 38.1°, 44.3°, 64.5°, and 77.4° can respectively assign to the refractive index of (111), (200), (220), and (311) planes, in accordance with the cubic structure of Ag crystals. One peak observed in the silicon at a 2θ position of 69.1° can be assigned to the (400) plane by the cubic structure of Si crystals. Figs. 3d and e present the reflectance spectra of plain silicon and pyramidal silicon, respectively. It is a clear indication that the pyramid silicon produced a gradual decrease in the refractive index between the surface of the silicon and the ambient air. Also, the Ag nanoparticles on the pyramidal silicon were also shown to reduce reflectivity, thereby allowing more of the light to be trapped, as shown in Fig. 3f.

In order to evaluate the importance of Ag nanoparticles on the different sizes of pyramid silicon can achieve high SERS response of the Raman marker molecule. Herein, the influence of texturing time on Raman intensity of rhodamine 6G (R6G, 10^{-8} M) investigated, as shown in Fig. 4. Immersion is generally used to adsorb organic molecules on SERS substrates; however, this typically requires deposition time on the scale of 6 h [24,25]. In this study, we used a spin coating to shorten the deposition time to just 3 min (2-min holding time and 1-min spin coating). As shown in Figs. 4a-d, longer texturing time was shown to increase the intensities of Raman signals corresponding to the vibrational modes of R6G from the in-plane vibration of C—H bond (1185 cm^{-1}) and aromatic C − C stretching vibrations (1311, 1360, 1507 and 1645 cm^{-1}) [13,26–29]. It was not unexpected, because any increase in the density of Ag nanoparticles on pyramidal silicon will increase the number of hot spots and thereby enhance SERS activity [30]. Extending the texturing time to 30 min led to a decrease in SERS

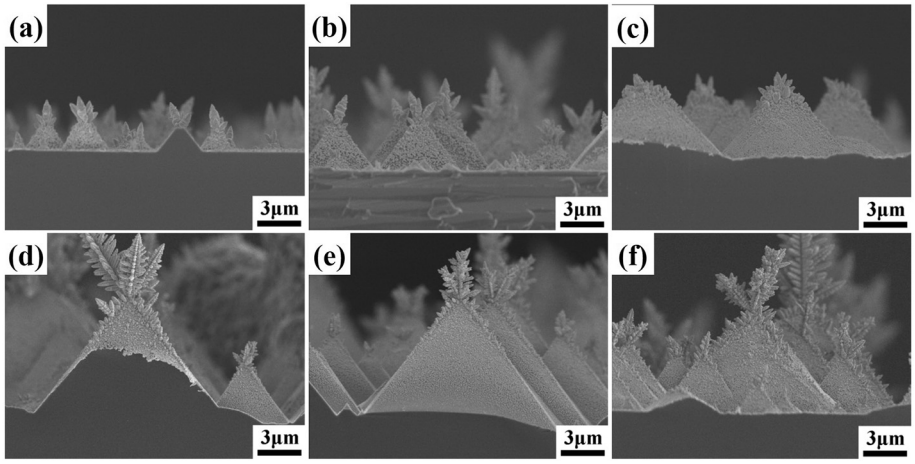

Fig. 2. Cross-sectional SEM images showing Ag nanoparticles deposited on pyramidal silicon that underwent wet texturing for periods of (a) 5, (b) 10, (c) 15, (d) 20, (e) 25, and (f) 30 min, respectively.

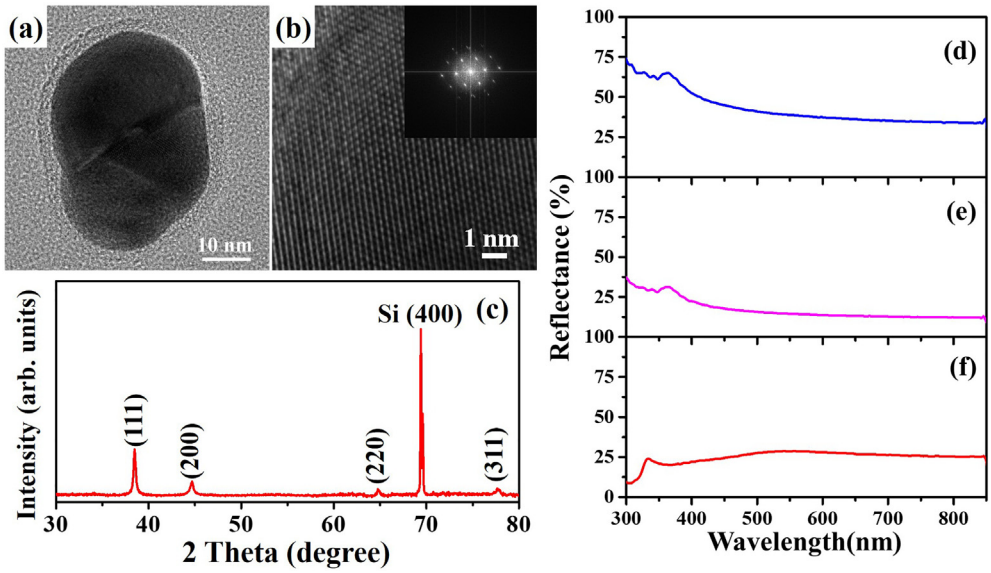

Fig. 3. (a) TEM image of Ag nanoparticle in Fig. 2(e); (b) HRTEM image of Ag nanoparticle in (a); (c) XRD pattern of Ag nanoparticles in Fig. 2(e); reflection spectra of (d) bare silicon, (e) pyramidal silicon (25 min), and (f) pyramid silicon (25 min) with Ag nanoparticles.

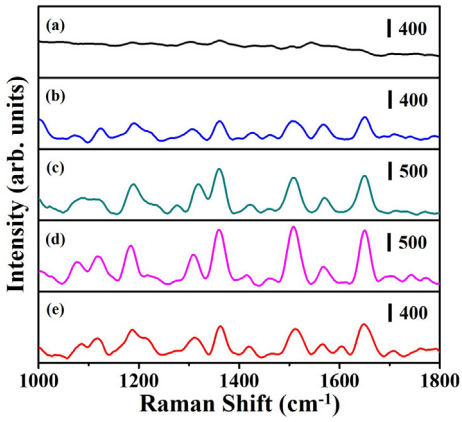

Fig. 4. SERS spectra of R6G solution (1×10^{-8} M) on pyramidal structures with Ag nanoparticles: texturing time of (a) 0, (b) 5, (c) 15, (d) 25, and (e) 30 min, respectively.

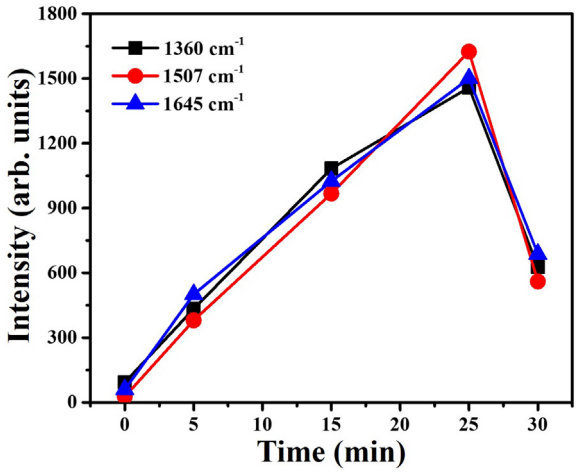

Fig. 5. SERS intensity of R6G peaks (Fig. 4) at 1360, 1507, and 1645 cm^{-1} as a function of the texturing time.

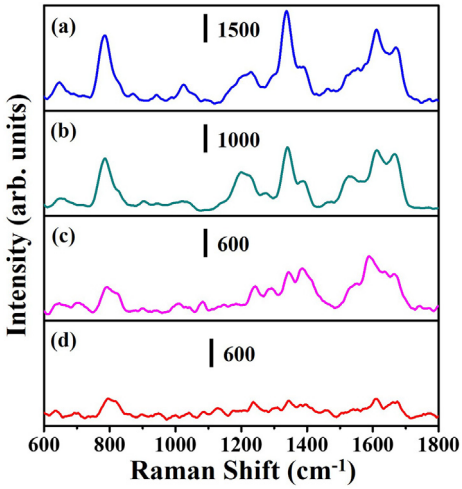

Fig. 6. SERS spectra from a 5-fluorouracil solution of various concentrations on a pyramidal silicon substrate with Ag nanoparticles (concentrations of the 5FU solution: 10^{-3}, 10^{-4}, 10^{-5}, and 10^{-6} M, respectively).

activity (Fig. 4e), which can attribute to the destruction of the pyramid structures and a reduction in the number of hot spots. Also, this phenomenon can be observed more clearly by comparing the intensity of the three Raman signal peaks at 1360, 1507, and 1645 cm^{-1} in Fig. 5. The silicon texturing time must be carefully controlled to ensure the high-density deposition of Ag nanoparticles to produce a large number of hot spots required to maximize the SERS effect.

We investigated the SERS properties of Ag nanoparticles on pyramid silicon using 5-fluorouracil (5-FU) as a probe molecule. 5-Fluorouracil (5-FU) is an antimetabolite of the pyrimidine analog type and a well-known anticancer drug widely used in the treatment of solid cancers, such as stomach, colon, lung, and breast cancers [31,32]. Fig. 6 presents the Raman spectra of 5-FU with Ag nanoparticles of various concentrations (10^{-3} to 10^{-6} M) on the pyramid silicon (texturing time of 25 min). The Raman signals corresponding to the vibrational modes of 5-FU are pyrimidine ring breath (786 cm^{-1}), ring plus C − F stretch (1235 cm^{-1}), ring plus C − H wag (1334 cm^{-1}), ring plus N − H wag (1399 cm^{-1}), and symmetric C═O stretches (1658 cm^{-1}), respectively. The SERS peaks of 5-FU increased gradually with the concentration of the 5-FU. Herein, we selected the band at 1658 cm^{-1} as the marker band for 5-FU due to its ideal peak profile. The intensity of the Raman peak at 1658 cm^{-1} dropped rapidly with a decrease in the concentration of 5-FU; however, it remained observable even at a 5-FU concentration of 10^{-6} M.

4. Conclusions

This paper describes a facile electroless deposition method for the growth of Ag nanoparticles on pyramidal silicon at room temperature with a reaction time of just 3 min. Our results indicate that the silicon texturing time must be carefully controlled to promote the growth of Ag nanoparticles at densities sufficient to produce hot spots suitable for SERS activity. The deposition of Ag nanoparticles on pyramid silicon was also shown to provide an excellent platform for the SERS detection of 5-FU (10^{-6} M), and could no doubt extend to other SERS sensing systems.

Acknowledgments

This study was supported financially by the Ministry of Science and Technology of Taiwan (MOST 106-2221-E-035-032-MY3). The authors appreciate the Precision Instrument Support Center of Feng Chia University in providing the fabrication and measurement facilities.

References

[1] P. Li, Y. Wei, Z. Zhao, X. Tan, J. Bian, Y. Wang, C. Lu, A. Liu, Highly efficient industrial large-area black silicon solar cells achieved by surface nanostructured modification, Appl. Surf. Sci. 357 (2015) 1830–1835.
[2] D.Z. Dimitrov, C.-H. Du, Crystalline silicon solar cells with micro/nano texture, Appl. Surf. Sci. 266 (2013) 1–4.
[3] B.-R. Huang, S.-C. Hung, C.-H. Hsu, C.-W. Tu, W.-L. Yang, Ultra-low reflection loss for silicon nanowire-array-textured based photovoltaic devices, Mater. Res. Bull. 80 (2016) 209–214.
[4] S.-Y. Lien, C.-H. Yang, C.-H. Hsu, Y.-S. Lin, C.-C. Wang, D.-S. Wuu, Optimization of textured structure on crystalline silicon wafer for heterojunction solar cell, Mater. Chem. Phys. 133 (2012) 63–68.
[5] P.-H. Tsai, H.-Y. Tsai, Fabrication and field emission characteristic of micro-crystalline diamond/carbon nanotube double-layered pyramid arrays, Thin Solid Films 584 (2015) 330–335.
[6] L.W. Veldhuizen, W.J.C. Vijselaar, H.A. Gatz, J. Huskens, R.E.I. Schropp, Textured and micropillar silicon heterojunction solar cells with hot-wire deposited passivation layers, Thin Solid Films 635 (2017) 66–72.
[7] M. Abbott, J. Cotter, Optical and electrical properties of laser texturing for high-efficiency solar cells, Prog. Photovolt. Res. Appl. 14 (2006) 225–235.
[8] R.A. Wind, H. Jones, M.J. Little, M.A. Hines, Orientation-resolved chemical kinetics: using microfabrication to unravel the complicated chemistry of KOH/Si etching, J. Phys. Chem. B 106 (2002) 1557–1569.
[9] M. Shikida, K. Sato, K. Tokoro, D. Uchikawa, Differences in anisotropic etching properties of KOH and TMAH solutions, Sensors Actuators A Phys. 80 (2000) 179–188.
[10] B.D. Choudhury, A. Abedin, A. Dev, R. Sanatinia, S. Anand, Silicon micro-structure and ZnO nanowire hierarchical assortments for light management, Opt. Mater. Express 3 (2013) 1039–1048.
[11] M. Abburi, T. Boström, I. Olefjord, Electrochemical isotropic texturing of mc-Si wafers in KOH solution, Mater. Chem. Phys. 139 (2013) 756–764.
[12] C. Barugkin, T. Allen, T.K. Chong, T.P. White, K.J. Weber, K.R. Catchpole, Light trapping efficiency comparison of Si solar cell textures using spectral photoluminescence, Opt. Express 23 (2015) A391–A400.
[13] C. Zhang, S.Z. Jiang, Y.Y. Huo, A.H. Liu, S.C. Xu, X.Y. Liu, Z.C. Sun, Y.Y. Xu, Z. Li, B.Y. Man, SERS detection of R6G based on a novel graphene oxide/silver nanoparticles/silicon pyramid arrays structure, Opt. Express 23 (2015) 24811–24821.
[14] Z. Li, S.C. Xu, C. Zhang, X.Y. Liu, S.S. Gao, L.T. Hu, J. Guo, Y. Ma, S.Z. Jiang, H.P. Si, High-performance SERS substrate based on hybrid structure of graphene oxide/AgNPs/Cu film@pyramid Si, Sci. Rep. 6 (2016) 38539.
[15] C. Zhang, B.Y. Man, S.Z. Jiang, C. Yang, M. Liu, C.S. Chen, S.C. Xu, H.W. Qiu, Z. Li, SERS detection of low-concentration adenosine by silver nanoparticles on silicon nanoporous pyramid arrays structure, Appl. Surf. Sci. 347 (2015) 668–672.
[16] S. Chen, B. Liu, X. Zhang, Y. Mo, F. Chen, H. Shi, W. Zhang, C. Hu, J. Chen, Electrochemical fabrication of pyramid-shape silver microstructure as effective and reusable SERS substrate, Electrochim. Acta 274 (2018) 242–249.
[17] C. Zhang, S.Z. Jiang, C. Yang, C.H. Li, Y.Y. Huo, X.Y. Liu, A.H. Liu, Q. Wei, S.S. Gao, X.G. Gao, B.Y. Man, Gold@silver bimetal nanoparticles/pyramidal silicon 3D substrate with high reproducibility for high-performance SERS, Sci. Rep. 6 (2016) 25243.
[18] J. Guo, S. Xu, X. Liu, Z. Li, L. Hu, Z. Li, P. Chen, Y. Ma, S. Jiang, T. Ning, Graphene oxide-ag nanoparticles-pyramidal silicon hybrid system for homogeneous, long-term stable and sensitive SERS activity, Appl. Surf. Sci. 396 (2017) 1130–1137.
[19] S. Jiang, J. Guo, C. Zhang, C. Li, M. Wang, Z. Li, S. Gao, P. Chen, H. Si, S. Xu, A sensitive, uniform, reproducible and stable SERS substrate has been presented based on MoS2@Ag nanoparticles@pyramidal silicon, RSC Adv. 7 (2017) 5764–5773.
[20] W. Ye, C. Shen, J. Tian, C. Wang, L. Bao, H. Gao, Self-assembled synthesis of SERS-active silver dendrites and photoluminescence properties of a thin porous silicon layer, Electrochem. Commun. 10 (2008) 625–629.
[21] C. Jing, Y. Fang, Simple method for electrochemical preparation of silver dendrites used as active and stable SERS substrate, J. Colloid Interface Sci. 314 (2007) 46–51.
[22] F. Bai, M. Li, P. Fu, R. Li, T. Gu, R. Huang, Z. Chen, B. Jiang, Y. Li, Silicon nanowire arrays coated with electroless Ag for increased surface-enhanced Raman scattering, APL Materials 3 (2015) 056101.
[23] E. Galopin, J. Barbillat, Y. Coffinier, S. Szunerits, G. Patriarche, R. Boukherroub, Silicon nanowires coated with silver nanostructures as ultrasensitive interfaces for surface-enhanced Raman spectroscopy, ACS Appl. Mater. Interfaces 1 (2009) 1396–1403.
[24] K. Zhao, J. Lin, L. Guo, ZnO/Ag porous nanosheets used as substrate for surface-enhanced Raman scattering to detect organic pollutant, RSC Adv. 5 (2015) 53524–53528.
[25] A.K. Samal, L. Polavarapu, S. Rodal-Cedeira, L.M. Liz-Marzán, J. Pérez-Juste, I. Pastoriza-Santos, Size tunable Au@Ag Core–Shell nanoparticles: synthesis and surface-enhanced Raman scattering properties, Langmuir 29 (2013) 15076–15082.
[26] S. Zaleski, M.F. Cardinal, D.V. Chulhai, A.J. Wilson, K.A. Willets, L. Jensen, R.P. Van Duyne, Toward monitoring electrochemical reactions with dual-wavelength SERS: characterization of rhodamine 6G (R6G) neutral radical species and covalent tethering of R6G to silver nanoparticles, J. Phys. Chem. C 120 (2016) 24982–24991.
[27] K. Zhang, T. Zeng, X. Tan, W. Wu, Y. Tang, H. Zhang, A facile surface-enhanced Raman scattering (SERS) detection of rhodamine 6G and crystal violet using au nanoparticle substrates, Appl. Surf. Sci. 347 (2015) 569–573.
[28] E. Kohr, B.I. Karawdeniya, J.R. Dwyer, A. Gupta, W.B. Euler, A comparison of SERS and MEF of rhodamine 6G on a gold substrate, Phys. Chem. Chem. Phys. 19 (2017) 27074–27080.

[29] C. Hou, G. Meng, Z. Huang, B. Chen, C. Zhu, Z. Li, Ordered arrays of vertically aligned Au-nanotubes grafted with flocky Au/Ag-nanospikes based on electrodeposition and subsequent redox reaction, Electrochem. Commun. 60 (2015) 104–108.
[30] A.E. Kandjani, M. Mohammadtaheri, A. Thakkar, S.K. Bhargava, V. Bansal, Zinc oxide/silver nanoarrays as reusable SERS substrates with controllable 'hot-spots' for highly reproducible molecular sensing, J. Colloid Interface Sci. 436 (2014) 251–257.
[31] Y. Abdel-Mottaleb, M.S.A. Abdel-Mottaleb, Molecular modeling studies of some uracil and new deoxyuridine derivatives, J. Chem. 2016 (2016) 5134732.
[32] C.O. Ehi-Eromosele, B.I. Ita, E.E.J. Iweala, Silica coated LSMO magnetic nanoparticles for the pH-responsive delivery of 5-fluorouracil anticancer drug, Colloids Surf. A Physicochem. Eng. Asp. 530 (2017) 164–171.